

Dynamics of the Critical Surface in High-Intensity Laser-Solid Interactions: Modulation of the XUV Harmonic Spectra

I. Watts, M. Zepf, E. L. Clark, M. Tatarakis, K. Krushelnick, and A. E. Dangor

The Blackett Laboratory, Imperial College of Science, Technology and Medicine, Prince Consort Road, London SW7 2BZ, United Kingdom

R. M. Allott, R. J. Clarke, D. Neely, and P. A. Norreys

Central Laser Facility, Rutherford Appleton Laboratory, Chilton, Didcot, Oxon OX11 0QX, United Kingdom

(Received 12 February 2001; published 27 March 2002)

The generation of harmonics from the interaction of an intense ($I \geq 10^{18}$ W cm $^{-2}$) laser with a solid surface is investigated. Modulation of the harmonic emission spectrum with a periodicity of 2 to 4 harmonics is observed at higher laser intensities. A similar modulation is predicted by a particle-in-cell simulation. The modulation is shown to be caused by the higher modes of oscillation of the critical surface during the interaction. As a result, the dynamics of the critical surface can be inferred from the shape of the harmonic spectrum.

DOI: 10.1103/PhysRevLett.88.155001

PACS numbers: 52.38.-r

The high intensities available with current lasers ($I > 10^{20}$ W cm $^{-2}$) have led to a wealth of novel phenomena observed in short pulse laser interactions with solids. These include the generation of relativistic electrons, beams of gamma rays, energetic protons (up to 50 MeV), and laser induced nuclear reactions [1–4]. The small spatial and temporal scales (≤ 10 μ m, ≤ 1 ps) make it difficult to diagnose these interactions in detail using conventional techniques. However, the higher harmonics of the fundamental laser frequency that are emitted can be a powerful diagnostic of the physical processes and plasma conditions in the interaction region [5–8]. The harmonic emission is also of interest as a bright source of coherent extreme ultraviolet (XUV) radiation. Using values of $I\lambda_0^2$ up to 10^{19} W cm $^{-2}$ μ m 2 , Norreys *et al.* [9] have observed the 75th harmonic of a 1.053 μ m laser with a conversion efficiency of 10^{-6} . The harmonic generation is due to electrons being dragged across the vacuum-solid interface by the electric field of the laser pulse. Harmonic generation can also be understood from a simple model based on the phase modulation experienced by the light upon reflection from the oscillating plasma-vacuum boundary [10–12].

In this paper we report the first observations of the modulated spectral structure of harmonics generated from solids. Our results show that at $I\lambda_0^2 \sim 10^{19}$ W cm $^{-2}$ μ m 2 the spectrum is modulated with a periodicity of 2 to 4 harmonics. The experimental results are compared to particle-in-cell (PIC) simulations which show that at high intensity the amplitude of the critical surface oscillation increases and is no longer purely sinusoidal at the laser frequency. We show that the modulation results directly from the motion of the reflecting surface. Good agreement is found when the trajectory of the critical surface, derived from PIC simulations, is used with the “moving mirror” model. Consequently, the dynamics of the critical surface can be inferred from the experimental observation of the

harmonic spectrum, and this may prove to be an important diagnostic technique in future high-intensity experiments.

The experiment was performed using the VULCAN laser system at the Rutherford Appleton Laboratory, delivering 0.7–1.0 ps pulses at 1.053 μ m with energies up to 50 J onto target. The rectangular beam, 20×11 cm 2 , was focused by an on-axis parabolic mirror ($f = 22$ cm). The target consisted of an optically polished fused silica slab set at a 45° angle of incidence with the beam p -polarized. The energy on target and pulse duration was monitored on a shot-to-shot basis. The focused intensity on target was estimated from the maximum ion energy in the blowoff plasma using CR39 nuclear track detectors [1,13,14] as well as from the γ -ray spectrum [4]. Another measure of the shot intensity was obtained from the hole boring velocity of the critical surface measured by the Doppler shift of the harmonics [5,15]. The combination of these techniques determined that the intensity on target was up to 1.0×10^{19} W cm $^{-2}$. The laser prepulse was determined in a previous experiment to be about 10^{-6} of the peak intensity. The subcritical plasma produced by this prepulse in front of the target was measured by optical probing and found to have a scale length which was typically less than 10 μ m [16].

The harmonic emission in the specularly reflected direction was observed by a slitless flat-field XUV spectrometer [17,18]. This consisted of a gold-coated cylindrical grazing-incidence collection mirror followed by a variable line-spaced grating, also at grazing incidence. The acceptance angle of the mirror and grating was 1×10^{-6} sr. The mirror and grating were oriented perpendicular to each other to produce an astigmatic line image in the detector plane of the harmonic emitting plasma at the target. The dispersed radiation was split into two wavelength regions and detected separately. The region 540–276 Å was intercepted by a plane gold-coated mirror set at 65° incidence and directed onto a double microchannel plate (MCP) detector coupled to an intensified optical 8-bit

charge-coupled device (CCD). The region 272–85 Å was detected by a back-thinned XUV sensitive 16-bit CCD detector. Thus harmonic emission from the 20th to 120th order could be detected simultaneously.

The absolute spectrometer response was calculated using the measured mirror reflectivities, the grating calibration [19], the transmission of any filters used, and the calibrated MCP/CCD detector response [20]. The conversion efficiency of each harmonic was calculated assuming uniform emission into 2π sr. This assumption is reasonable in view of previous measurements [9,21].

A typical spectrum showing the 20th (526.5 Å) to 37th (284.6 Å) harmonics and corrected for the spectrometer response and background is shown Fig. 1a. The highest harmonic observed was the 60th at 175.5 Å. The conversion efficiency varied from 4.6×10^{-6} at the 20th harmonic and, interpolating between the two detectors, to $\sim 4.0 \times 10^{-8}$ at the 60th. The harmonic spectrum shows modulations at every 2 to 4 harmonics over the entire range on both detectors. It should be noted that the modulations peak at different harmonics for different shots and are observed throughout the entire spectral range. Figure 1b shows a typical harmonic spectrum at a lower intensity. This shows harmonics only up to the 30th at 351.0 Å. Comparing Figs. 1a and 1b, it is clear that the modulations in the harmonic spectra are much reduced and that

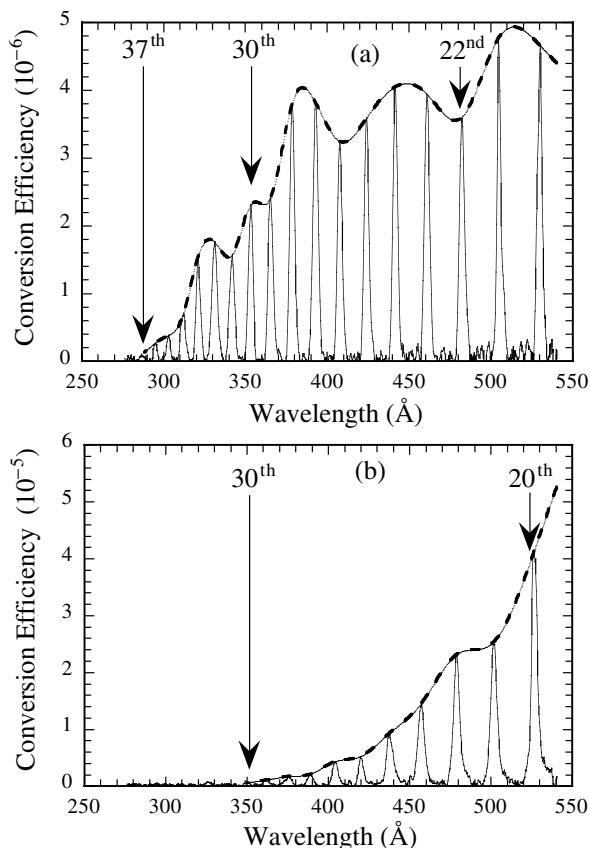


FIG. 1. Lineouts of typical harmonic spectra for (a) high intensity $I\lambda_o^2 \sim 10^{19} \text{ W cm}^{-2} \mu\text{m}^2$ and (b) low intensity $I\lambda_o^2 \sim 10^{18} \text{ W cm}^{-2} \mu\text{m}^2$.

the structure is an intensity dependent effect. The stronger modulations correspond to a higher incident intensity.

The maximum ion energies E_{max} and the average value of the Doppler shift $\Delta\lambda_o/\lambda_o$ for the two shots are shown in Table I. The scaling for the maximum ion energy $E_{\text{max}} \sim (I\lambda_o^2)^{0.5}$ as established empirically in Refs. [1,13,14] was used. The Doppler shift also scales as $(I\lambda_o^2)^{0.5}$, for $I\lambda_o^2 \geq 10^{18} \text{ W cm}^{-2} \mu\text{m}^2$, as proposed by Wilks *et al.* [15] and experimentally confirmed by Zepf *et al.* [5]. Below this value a transition from hole-boring to plasma expansion occurs which results in a change from a redshift to a blueshift of the harmonics. The inferred intensities are also shown in Table I.

The PIC code used in this paper was developed by Pfund and Lichters and is described in Refs. [11] and [22]. It is a fully relativistic one-dimensional code, with oblique incidence treated by transformation to a moving frame of reference in which the light is normally incident [23,24]. For the simulations here a p -polarized laser beam is incident at 45° onto a one wavelength thick plasma slab with density $n_e/n_c = 13$ (where n_e is the electron density and n_c is the critical density at the laser wavelength λ_o). The pulse had a sine-squared temporal profile and a duration of 20 laser cycles. Simulations were performed with both mobile and immobile ions without affecting the results significantly.

The PIC simulations exhibit a similar modulation structure to that observed experimentally with a modulation amplitude which increases with higher intensity. This has previously been reported in PIC simulations by Lichters *et al.* [22] where the spectrum was found to be modulated with a periodicity of ~ 10 harmonics. The modulations were ascribed to internal reflections of transmitted light due to the finite size of the plasma slab. This hypothesis was tested here by performing simulations with various thicknesses of plasma slabs, and this was found to have no effect on the modulation structure. This suggests that the modulation structure is intrinsic to the harmonic generation and not related to internal propagation and reflection of harmonic light.

Figure 2 shows the simulated harmonic spectra of the reflected light for high and low $I\lambda_o^2$ similar to the experimental values in Fig. 1. At the lower value of $I\lambda_o^2$ (Fig. 2b) the conversion into harmonics is low with a smooth unmodulated roll-off. The noise in the spectra is numerical and is reduced when using a higher temporal resolution. The highest harmonic above noise in the simulation is the 6th. In the experiment up to the 30th harmonic could be observed at the same value of $I\lambda_o^2$. At the higher value of $I\lambda_o^2$ (Fig. 2a) the harmonic emission is enhanced and the spectrum is modulated at every 4 to 5 harmonics. This is to be compared to the 2 to 4 harmonics observed experimentally. The highest harmonic above numerical noise in this case is the 55th.

The oscillatory motion of the critical density surface $x(t)$ for the two simulations is shown in Fig. 3. The motion is periodic at the laser frequency ω_o and the displacement is approximately 3 times larger for higher $I\lambda_o^2$. The

TABLE I. Inferred values of $I\lambda_o^2$ for the two shots of Fig. 1.

Shot number	Maximum proton energies		Wavelength shift (hole boring)	
	E_{\max} (MeV)	$(I\lambda_o^2)_{CR39}$ ($\text{W cm}^{-2} \mu\text{m}^2$)	$\Delta\lambda_o/\lambda_o$	$(I\lambda_o^2)_{HB}$ ($\text{W cm}^{-2} \mu\text{m}^2$)
270502 (Fig. 1a)	11.0	1×10^{19} ($\pm 30\%$)	0.007 ± 0.0008	1×10^{19} ($\pm 20\%$)
290502 (Fig. 1b)	6.5	2×10^{18} ($\pm 30\%$)	-0.001 ± 0.0003	$\sim 1 \times 10^{18}$ ($\pm 20\%$)

oscillatory mode at ω_o is due to the electromagnetic force at the laser frequency and that at $2\omega_o$ is due to the ponderomotive force. These modes are apparent in the power spectrum of Fig. 3b at the lower value of $I\lambda_o^2$. Some energy is coupled to modes greater than $2\omega_o$ by nonlinearities. Lichters *et al.* [11] found that these additional modes must be included in the description of $x(t)$ to reproduce the conversion efficiencies observed in the PIC simulations. As $I\lambda_o^2$ increases, higher surface modes are excited with increasing amplitudes as shown in Fig. 3a. The modes at $4\omega_o$ and $5\omega_o$ become larger and affect the motion of the critical surface significantly.

In order to interpret the PIC results we include in the moving-mirror model all the oscillatory modes present in $x(t)$ rather than using arbitrary components at ω_o , $2\omega_o$, and $4\omega_o$ as done by Lichters *et al.* [11]. This is done by calculating the waveform of the reflected light numeri-

cally with the function $x(t)$ taken from the PIC simulation (Figs. 3a and 3b). The calculated spectrum of the harmonics for the low and high values of $I\lambda_o^2$ are shown in Fig. 3c. The spectra show the same intensity dependence of the modulation structure as observed experimentally.

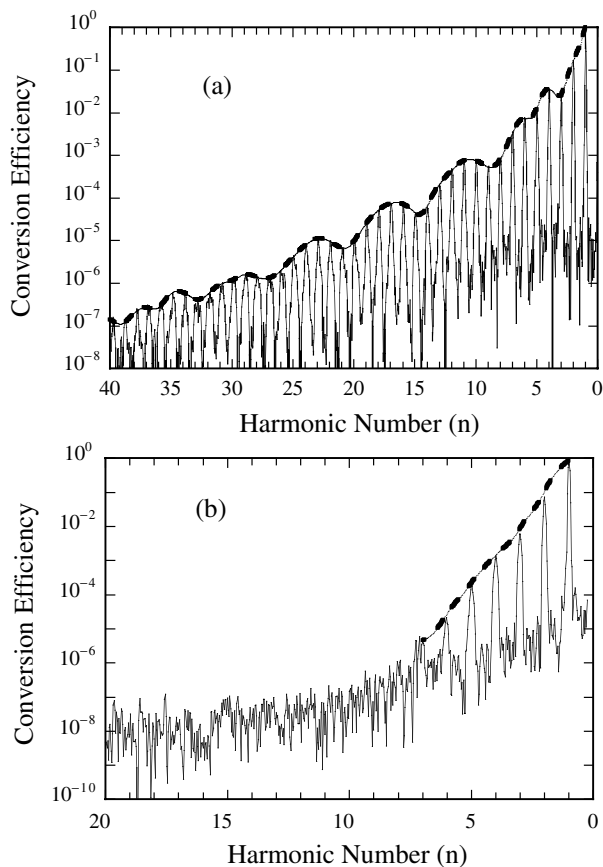


FIG. 2. The simulated harmonic spectra for (a) $I\lambda_o^2 = 1.23 \times 10^{19} \text{ W cm}^{-2} \mu\text{m}^2$ and (b) $I\lambda_o^2 = 1.37 \times 10^{18} \text{ W cm}^{-2} \mu\text{m}^2$. The conversion efficiency is given by $2|E(\omega)/E_L|^2$.

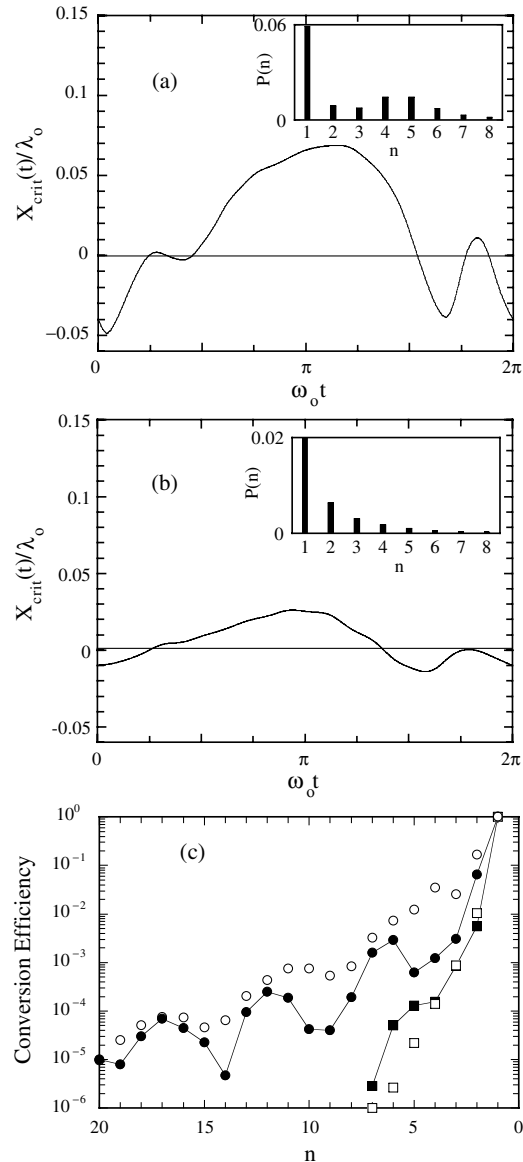


FIG. 3. The motion of the critical surface $x(t)$ from the simulations for (a) $I\lambda_o^2 = 1.23 \times 10^{19} \text{ W cm}^{-2} \mu\text{m}^2$ and (b) $I\lambda_o^2 = 1.37 \times 10^{18} \text{ W cm}^{-2} \mu\text{m}^2$. Inset shows the different modes of oscillation. (c) Calculated conversion into harmonics using the oscillating mirror model. Closed circles correspond to $I\lambda_o^2 = 1.23 \times 10^{19} \text{ W cm}^{-2} \mu\text{m}^2$ and closed squares correspond to $I\lambda_o^2 = 1.37 \times 10^{18} \text{ W cm}^{-2} \mu\text{m}^2$. The open symbols show the PIC simulation results of Fig. 2 for comparison.

Furthermore, the shape of the spectrum is in good quantitative agreement with the PIC simulations. This illustrates that the moving-mirror model captures the essential physics of the harmonic generation process.

We have also taken the Fourier transform of the calculated harmonic spectra and compared this to the motion of the critical surface from the PIC simulations. The amplitude of the critical surface motion and the degree of nonlinearity of the original oscillation is consistent with the Fourier transform. Consequently, the modulation of observed harmonic spectra may be used to determine the dynamics of the critical surface in future experiments. However, this was not done using the experimentally observed spectra in Fig. 1 since only part of the spectrum was measured in this work (i.e., that in the soft x-ray/XUV region). Also phase information of the harmonics is lost in the intensity measurements.

In the simulations the modulations are greatly suppressed by the addition of a linear density ramp to the slab profile. For this case the conditions were the same as in Fig. 2a, with $I\lambda_p^2 = 1.23 \times 10^{19} \text{ W cm}^{-2} \mu\text{m}^2$, except that now the density rises from zero to $n_e/n_c = 10$ over 0.5 wavelengths. The modulation structure of Fig. 2a is now not apparent in the harmonic spectrum. The absence of any modulation structure demonstrates that this effect depends on initial scale length as well as the incident intensity. The PIC simulation shows that now no single critical surface exists and that layers of ablating plasma gives rise to multiple overdense reflecting layers. Even at lower intensities it has been shown analytically by Kingham *et al.* [25] that the reflection of the incident wave is no longer localized at the critical surface in the presence of a ramp and regions above critical density can also contribute to the generation of the harmonic spectrum [22]. For the experimental conditions considered in this paper the scale length prior to the arrival of the laser pulse is typically in the range of 1–6 μm . This is in contrast to the sharp plasma discontinuity that is implicit in the moving mirror model. It is therefore surprising that the moving mirror model and the PIC simulations using a step profile agree so closely with the experimental observations. However, the large laser pressures can lead to significant steepening of the density profile [15] if the pulse is sufficiently long. At the same time, the laser expels plasma from the focal region, creating the kind of vacuum-plasma boundary that is required to produce the modulation structure. That this is indeed the case has been shown previously by investigating the conversion efficiency at different prepulse levels [6]. For short pulse lengths a rapid drop of the conversion efficiency with increasing prepulse was observed. By contrast, experiments with ~ 1 ps pulses [9] were insensitive to the level of prepulse and showed conversion efficiencies in good agreement with PIC simulations for short or steplike density profiles. The modulation structure should

therefore be a good indicator of high contrast ratios for shorter duration laser pulses ($\lesssim 200$ fs).

To summarize, the experimentally observed modulation of the harmonic spectrum agrees with the PIC simulation—although clearly for these experiments a fully three-dimensional simulation will be required to find precise agreement. The observed modulation is due to the introduction of higher modes of oscillation of the critical surface $x(t)$ and can be described in terms of the moving mirror model. Observations of the modulational structure of harmonic emission from high-intensity interactions may be important as a diagnostic tool of the behavior of the critical surface in future experiments, for example, in “fast ignitor” type experiments. Measurements of the modulational structure of harmonic emission from several different angles can provide three-dimensional information on the critical surface dynamics under intense laser irradiation. Understanding this effect may also be important for determining the suitability of this XUV source for future applications.

The authors are indebted to Professor J. Meyer-ter-Vehn for the use of the PIC simulation software. The work was supported by the United Kingdom Engineering and Physical Sciences Research Council (EPSRC).

-
- [1] E. L. Clark *et al.*, Phys. Rev. Lett. **85**, 1654 (2000).
 - [2] S. P. Hatchett *et al.*, Phys. Plasmas **7**, 2076 (2000).
 - [3] M. I. K. Santala *et al.*, Appl. Phys. Lett. **78**, 19 (2001).
 - [4] K. W. D. Ledingham *et al.*, Phys. Rev. Lett. **84**, 899 (2000).
 - [5] M. Zepf *et al.*, Phys. Plasmas **3**, 3242 (1996).
 - [6] M. Zepf *et al.*, Phys. Rev. E **58**, R5253 (1998).
 - [7] R. Hassner *et al.*, Opt. Lett. **22**, 1491 (1997).
 - [8] W. Theobald *et al.*, Phys. Rev. Lett. **77**, 298 (1996).
 - [9] P. A. Norreys *et al.*, Phys. Rev. Lett. **76**, 1832 (1996).
 - [10] S. V. Bulanov, N. M. Naumova, and F. Pegoraro, Phys. Plasmas **1**, 745 (1994).
 - [11] R. Lichters, J. Meyer-ter-Vehn, and A. Pukhov, Phys. Plasmas **3**, 3425 (1996).
 - [12] D. von der Linde and K. Rzazewski, Appl. Phys. B, Lasers Opt. **63**, 499 (1996).
 - [13] F. N. Beg *et al.*, Phys. Plasmas **4**, 447 (1997).
 - [14] A. P. Fews *et al.*, Phys. Rev. Lett. **73**, 1801 (1994).
 - [15] S. C. Wilks *et al.*, Phys. Rev. Lett. **69**, 1383 (1992).
 - [16] M. I. K. Santala *et al.*, Phys. Rev. Lett. **84**, 1459 (2000).
 - [17] D. Neely *et al.*, Rutherford Appleton Laboratory Technical Report No. RAL-TR-95-025, 1995, p. 113.
 - [18] D. Neely *et al.* (to be published).
 - [19] D. Neely and D. M. Chambers, Rutherford Appleton Laboratory Technical Report No. RAL-TR-96-74, 1997.
 - [20] M. Zepf *et al.*, Rutherford Appleton Laboratory Technical Report No. RAL-TR-95-025, 1995, p. 115.
 - [21] D. M. Chambers *et al.*, Opt. Commun. **148**, 289 (1998).
 - [22] R. Lichters and J. Meyer-ter-Vehn, Inst. Phys. Conf. Ser. **154**, 221 (1997).
 - [23] A. Bourdier, Phys. Fluids **26**, 1804 (1983).
 - [24] A. R. Bell, Astrophys. Space Sci. **256**, 13 (1998).
 - [25] R. Kingham *et al.*, Phys. Rev. Lett. **86**, 810 (2001).